Analysis of 316L Stainless Steel Powder Bed Fusion Material

Research and Development Office
Science and Technology Program
Final Report No. ST-2021-19085-3, TM-8540-2021-017

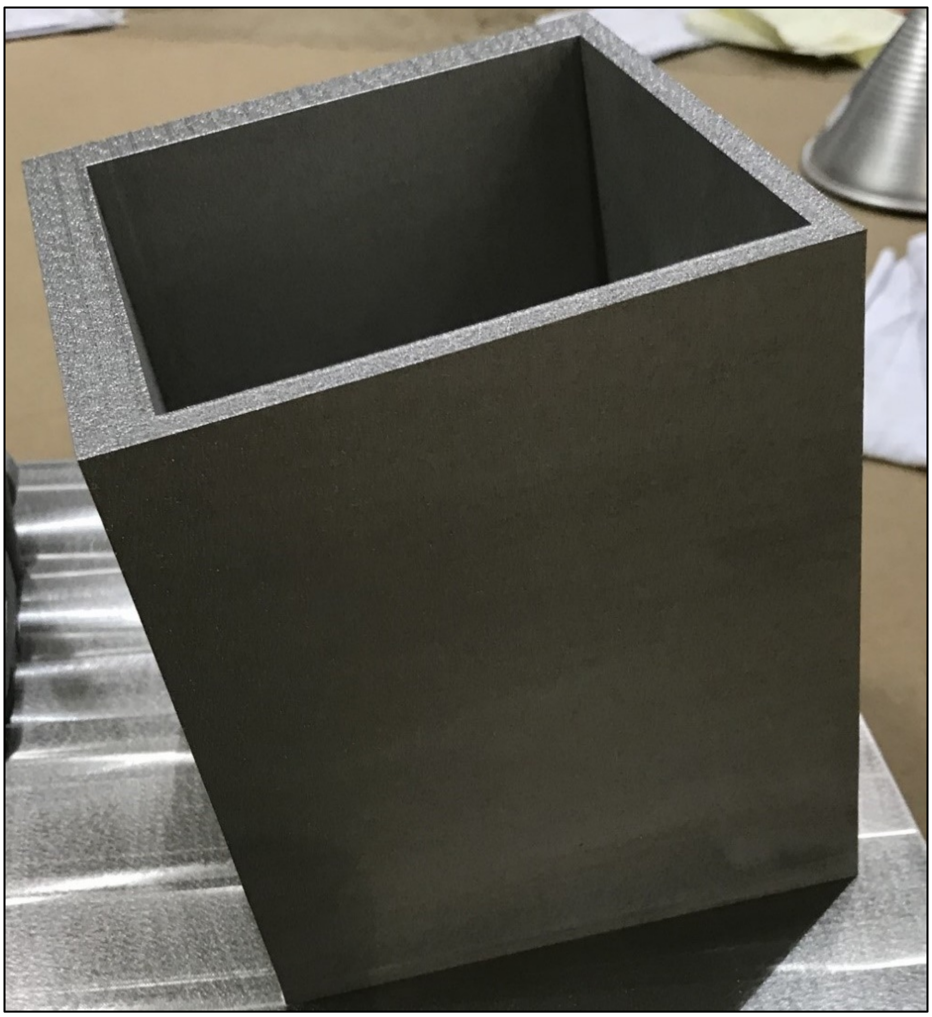

U.S. Department of the Interior September 2021

REPORT DOCUMENTATION PAGE

Form Approved
OMB No. 0704-0188

1. REPORT DATE *(DD-MM-YYYY)*	2. REPORT TYPE	3. DATES COVERED *(From - To)*
September 2021	Research, Final Report	2019–2021

4. TITLE AND SUBTITLE
Analysis of 316L Stainless Steel Powder Bed Fusion Material

5a. CONTRACT NUMBER
XXXR4524KS
RR4888FARD1901801

5b. GRANT NUMBER

5c. PROGRAM ELEMENT NUMBER
1541 (S&T)

6. AUTHOR(S)
Matthew Jermyn mjermyn@usbr.gov
Grace Weber gweber@usbr.gov
Stephanie Prochaska sprochaska@usbr.gov
David Tordonato dtordonato@usbr.gov

5d. PROJECT NUMBER
Final Report No. ST-2021-19085-3

5e. TASK NUMBER

5f. WORK UNIT NUMBER
86-68540

7. PERFORMING ORGANIZATION NAME(S) AND ADDRESS(ES)
David Tordonato
Materials and Corrosion Laboratory
Technical Service Center
Bureau of Reclamation
U.S. Department of the Interior
PO Box 25077, Denver Federal Center
Denver CO 80225-0007

8. PERFORMING ORGANIZATION REPORT NUMBER
8540-2021-017

9. SPONSORING/MONITORING AGENCY NAME(S) AND ADDRESS(ES)
Science and Technology Program
Research and Development Office
Bureau of Reclamation
U.S. Department of the Interior
PO Box 25007, Denver Federal Center
Denver, CO 80225-0007

10. SPONSOR/MONITOR'S ACRONYM(S)
R&D: Research and Development Office
Reclamation: Bureau of Reclamation
DOI: U.S. Department of the Interior

11. SPONSOR/MONITOR'S REPORT NUMBER(S)
Final Report No. ST-2021-19085-3

12. DISTRIBUTION/AVAILABILITY STATEMENT
Final report may be downloaded from https://www.usbr.gov/research/projects/index.html

13. SUPPLEMENTARY NOTES

14. ABSTRACT
This final report is an analysis of Powder Bed Fusion (PBF) stainless steel 316L and its suitability for Bureau of Reclamation (Reclamation) purposes. An open cube was printed using PBF additive manufacturing. Test specimens were sectioned from the cube and analyzed for mechanical properties, density, and microstructure. The PBF process achieved high dimensional accuracy to the computer-aided design model. A small amount of porosity was observed, and the material had a lower toughness than wrought 316L. Overall, a reduced performance was due to anisotropy, which was most notable in the direction transverse to print layer deposition. With consideration to build orientation, the PBF process, when used with appropriate starting material and process parameters, may be an acceptable candidate for production of components depending on service.

15. SUBJECT TERMS
Additive manufacturing, 3D printing, aging infrastructure, corrosion mitigation, remote monitoring, fabrication

16. SECURITY CLASSIFICATION OF:			17. LIMITATION OF ABSTRACT	18. NUMBER OF PAGES	19a. NAME OF RESPONSIBLE PERSON
a. REPORT	b. ABSTRACT	THIS PAGE		48	David Tordonato
U	U	U			19b. TELEPHONE NUMBER *(Include area code)* 303-445-2394

Standard Form 298 (Rev. 8/98)
Prescribed by ANSI Std. Z39.18

Analysis of 316L Stainless Steel Powder Bed Fusion Material

prepared by

Technical Service Center
Matthew Jermyn, Materials Engineer
Grace Weber, Materials Engineer
Stephanie Prochaska, Materials Engineer
David Tordonato, Materials Engineer

Cover Photograph: A 5- by 5-inch open cube after powder bed fusion build, prior to separation from build plate (Concurrent Technologies).

Mission Statements

The U.S. Department of the Interior protects and manages the Nation's natural resources and cultural heritage; provides scientific and other information about those resources; and honors its trust responsibilities or special commitments to American Indians, Alaska Natives, and affiliated Island Communities.

The mission of the Bureau of Reclamation is to manage, develop, and protect water and related resources in an environmentally and economically sound manner in the interest of the American public.

Disclaimer

Information in this report may not be used for advertising or promotional purposes. The data and findings should not be construed as an endorsement of any product or firm by the Bureau of Reclamation, U.S. Department of Interior, or Federal Government. The products evaluated in the report were evaluated for purposes specific to the Bureau of Reclamation mission. Reclamation gives no warranties or guarantees, expressed or implied, for the products evaluated in this report, including merchantability or fitness for a particular purpose.

Acknowledgements

The Science and Technology Program, Bureau of Reclamation, sponsored this research.

Peer Review

Bureau of Reclamation
Technical Service Center
Materials and Corrosion Laboratory Group

Technical Memorandum No. 8540-2021-017

Analysis of 316L Stainless Steel Powder Bed Fusion Material

MATTHEW JERMYN
Digitally signed by MATTHEW JERMYN
Date: 2021.10.28 09:04:27 -06'00'

Prepared by: Matthew Jermyn
Materials Engineer, Materials and Corrosion Laboratory, 86-68540

GRACE WEBER
Digitally signed by GRACE WEBER
Date: 2021.10.28 14:43:40 -06'00'

Checked by: Grace Weber
Materials Engineer, Materials and Corrosion Laboratory, 86-68540

STEPHANIE PROCHASKA
Digitally signed by STEPHANIE PROCHASKA
Date: 2021.10.28 15:03:37 -06'00'

Technical Approval by: Stephanie Prochaska, M.S.
Materials Engineer, Materials and Corrosion Laboratory, 86-68540

Digitally signed by BRYAN HEINER
Date: 2021.10.29 13:05:20 -06'00'

Peer Review by: Bryan Heiner
Hydraulic Engineer, Hydraulic Investigations and Laboratory Services, 86-68560

Acronyms and Abbreviations

3D	three-dimensional
AM	additive manufacturing
ASTM	ASTM International, formerly American Society for Testing and Materials
HRB	Hardness Rockwell B
PBF	powder bed fusion
PM	powder metallurgy
SLM	selective laser melting
Reclamation	Bureau of Reclamation
UTS	ultimate tensile strength

Symbols and Measurements

%	percent
psi	pounds per square inch
in	inch
in^2	square inch
lb	pound

Contents

Appendices

Tables

Figures

Executive Summary

This final report is an analysis of Powder Bed Fusion (PBF) stainless steel 316L and its suitability for Bureau of Reclamation (Reclamation) purposes.

A 5- by 5-inch open cube was printed using PBF additive manufacturing. A three-dimensional laser scan of the cube showed that the PBF process achieved high dimensional accuracy to the computer-aided design model. Test samples were sectioned from the cube and analyzed for microstructure, density, and mechanical properties.

Microstructural analysis showed a small amount of porosity in the micrographs while no impurities were observed within the material. Density results were within the 96 to 97 percent dense range for all but one sample. Tensile testing showed the average yield stress of the PBF samples was higher than the average yield strength of the wrought material; however, impact testing showed that the material exhibited a lower toughness than wrought material. Anisotropy was observed in the direction transverse to print layer deposition, displaying an overall reduced material performance.

With consideration of the above findings, the PBF process, when used with appropriate starting material and process parameters, may be an acceptable candidate for production of components depending on application. Consideration should be given to the orientation of components in the build process as material performance was observed to be anisotropic and, therefore, the appropriateness for use may require assessment on a case-by-case basis.

Introduction

Background

The Bureau of Reclamation (Reclamation) undertook a study to investigate and demonstrate the capabilities of additive manufacturing (AM) for hydropower applications. The study was broken into two phases. Phase 1 investigates three AM techniques of interest thus to evaluate the processes and resulting material properties—Direct Energy Deposition, Laser Powder Bed Fusion, and Cold Spray. Phase 2 presents three case studies in which a component of interest is reproduced using knowledge gained during phase 1.

This final report focuses specifically on the investigation and analysis of 316L stainless steel powder bed fusion (PBF) material and is intended to be incorporated into the larger context of AM for hydropower applications, which will be presented as Final Report No. ST-2021-19085-1, Technical Memorandum No. 8540-2021-015.

316L Stainless Steel and the Powder Bed Fusion Process

With the rise of AM technologies, there is a need to evaluate and compare new additively manufactured materials against their traditionally produced counterparts. This report will provide an analysis of PBF-produced 316L stainless steel in comparison with wrought material.

To provide a test part for the analysis, a 5- by 5-inch open cube was printed from 316L stainless steel powder using the PBF process, specifically selective laser melting (SLM) on a SLM 280^{HL} machine (figures 1 and 2) in an argon environment. The completed cube can be seen in figures 3 and 4. The Powder Feedstock Documentation can be found in appendix A.

The performance and characteristics of the printed material were assessed with metallography, density measurement, hardness testing, tensile testing, fractography, and impact testing on samples machined from the cube.

Figure 1.—SLM 280^{HL} machine used to build a 5- by 5-inch open cube with 316L stainless steel powder. Photograph courtesy of Concurrent Technologies.

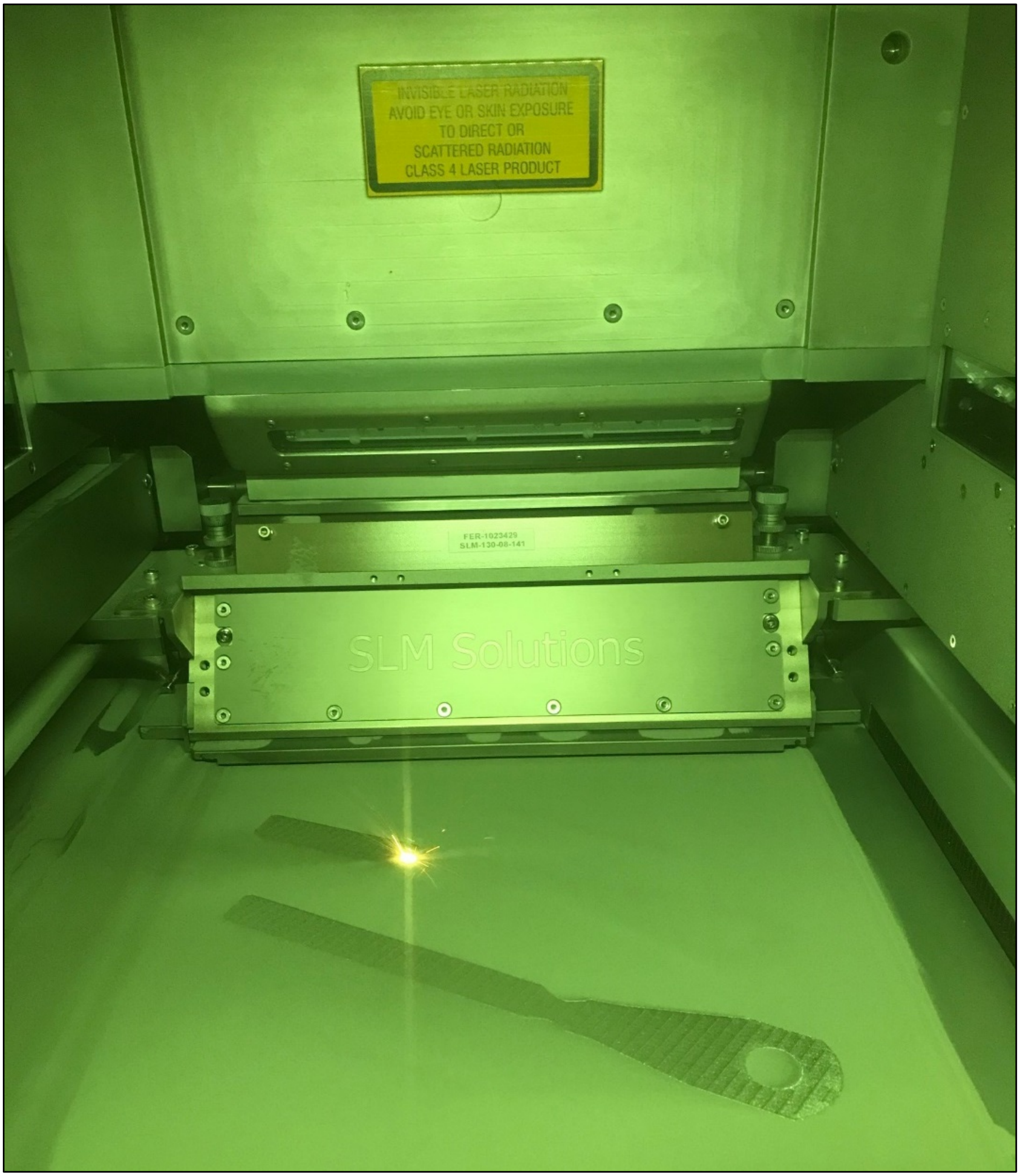

Figure 2.—Interior of SLM 280HL machine with a build in progress. Note that the component being built is not the test cube of this current study. Photograph courtesy of Concurrent Technologies.

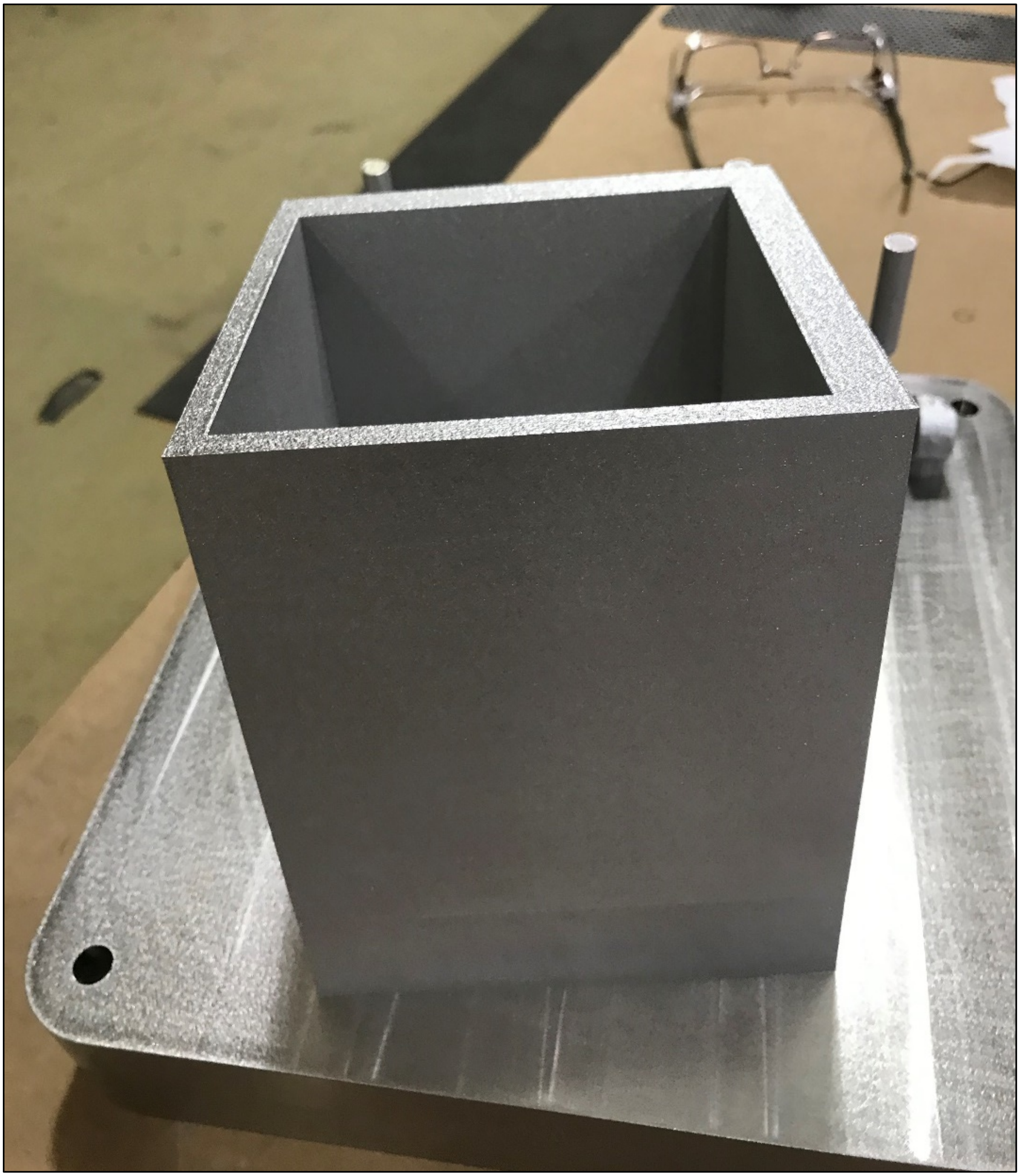

Figure 3.—The 5- by 5-inch open cube after PBF build, prior to separation from build plate. Photograph courtesy of Concurrent Technologies.

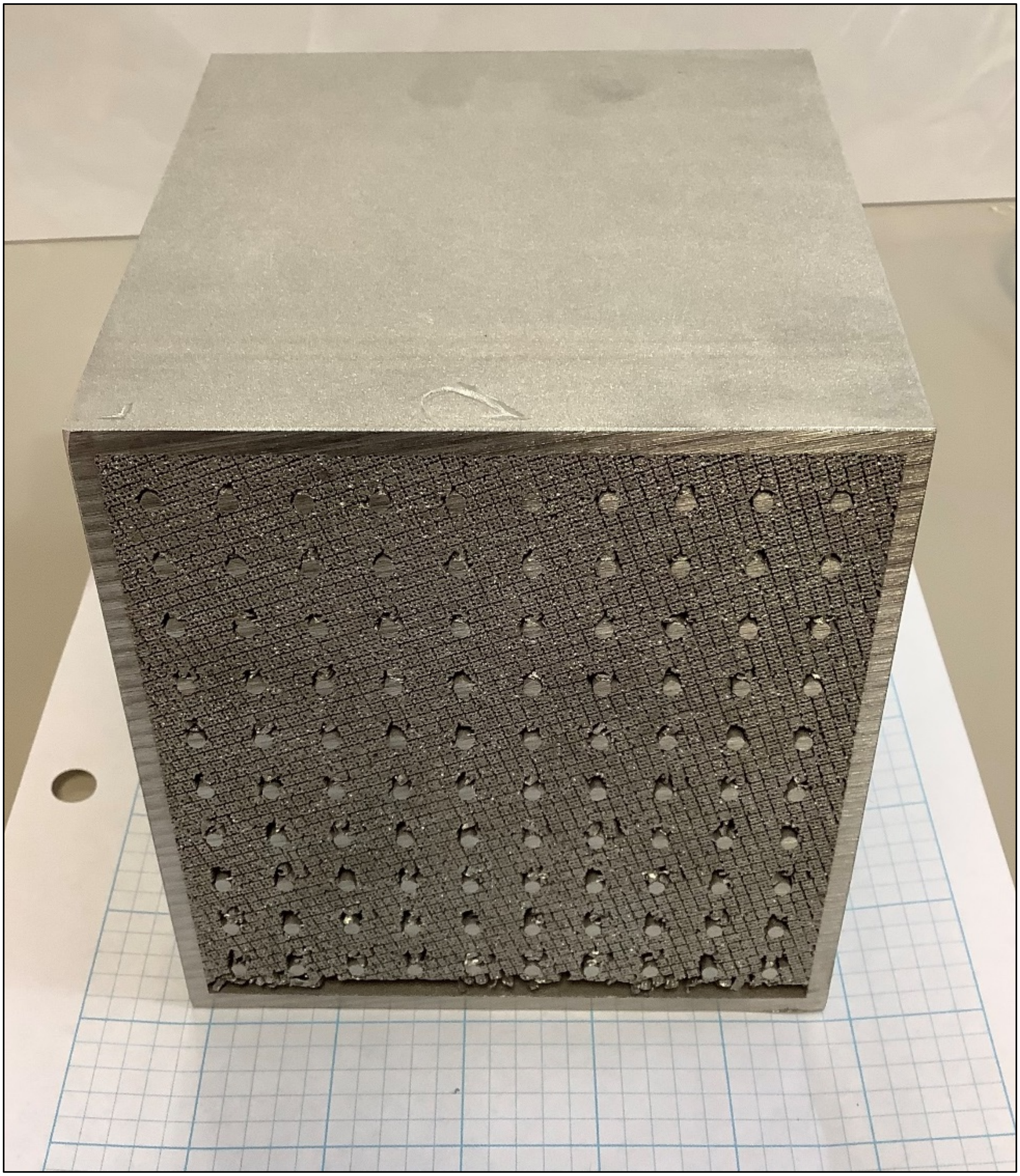

Figure 4.—Underside of the 5- by 5-inch open cube after separation from build plate. The support material is visible (Reclamation/David Tordonato).

Methodology

Researchers chose the open cube design to allow comparison of material properties in each of the three primary printing directions (X, Y, and Z). To assess the impact of thermal processes on the material properties, the print included two vertical wall thicknesses—0.50 and 0.25 inch. Note a thicker cross section would theoretically have a higher heat input and slower cooling rate than a thinner cross section.

The cube was constructed using 50-micron build layers and recycled 316L stainless steel powder, spherical and 15 to 45 microns in diameter. For assessment of the as-printed material, there was no post-build heat treatment or stress relief. The part was built at a slight angle using support material to prevent the internal stresses (developed during the rapid heating and cooling of the material) from causing the part to separate from the build plate. The entire build was comprised of 3,082 layers with a build time of 75 hours. No post-process machining was performed by the vendor. The part was scanned using a three-dimensional (3D) laser scanner to provide dimensional comparison to the original model. The 3D Laser Scan Results are included in appendix B.

After visual inspection and 3D scanning, samples for destructive testing were machined from each of the sides to assess material properties and evaluate process suitability. Metallography, density measurement, hardness testing, tensile testing, fractography, and impact testing were performed as part of this study. Sample locations and labels can be seen in figure 5. Label nomenclature can be found in tables 1 through 3. Similar tests were conducted with purchased 316L wrought material for comparison.

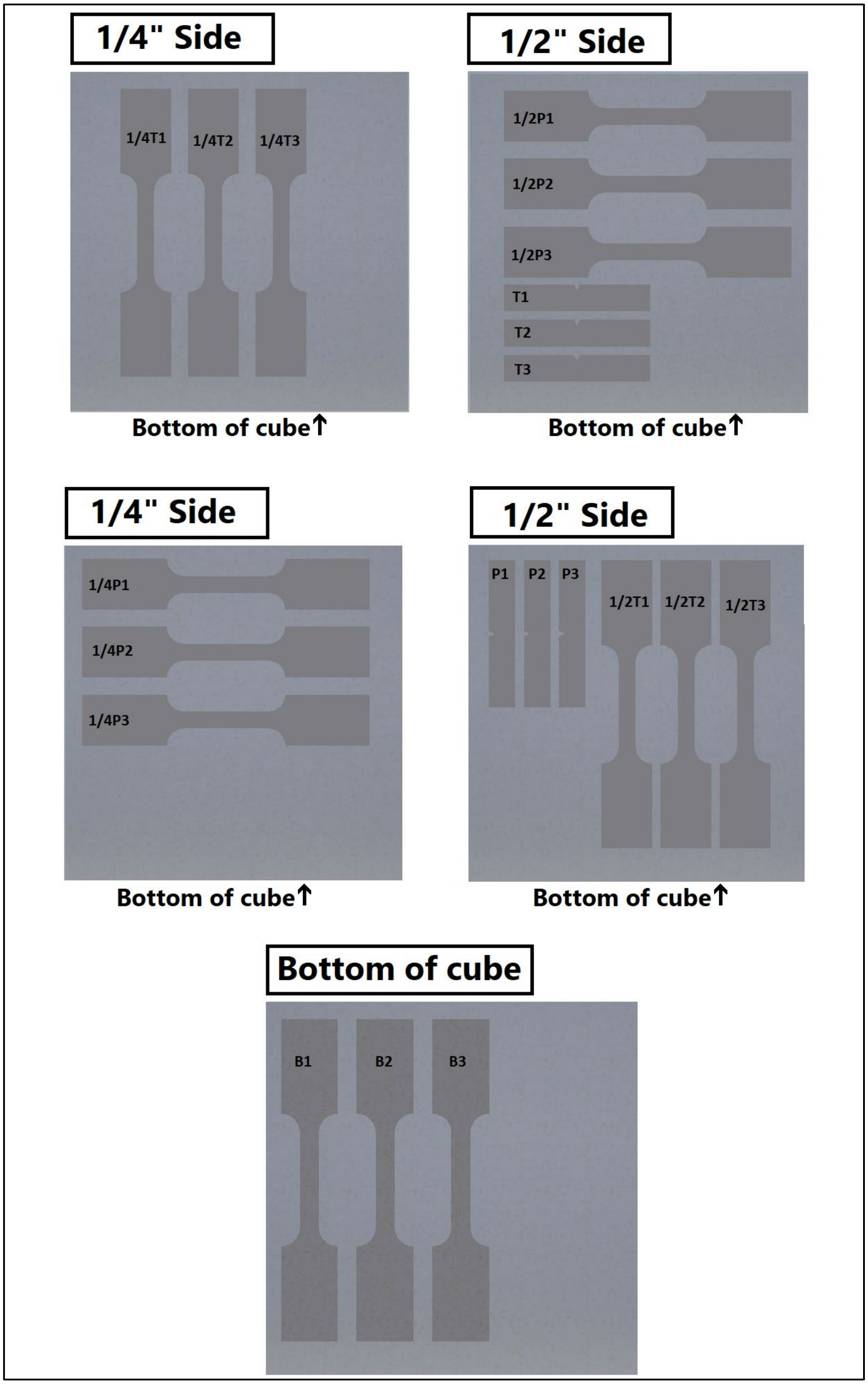

Figure 5.—Identification of samples taken from the test cube.

Metallographic Analysis

Metallography samples were taken from the grip portions of tested tensile samples. The nomenclature identifying the samples (table 1) indicates the orientation of the tensile sample used and the plane being viewed (figure 6).

Table 1.—Metallographic Sample Identification Nomenclature

First Digit Wall Designation	Second Digit Sample Orientation	Third Digit Sample Number	Fourth Digit Plane Being Viewed
B = Bottom plate 1/2 = 1/2-inch wall 1/4 = 1/4-inch wall	T = Transverse P = Parallel	Unique and sequential identification	F = Face X = Cross section

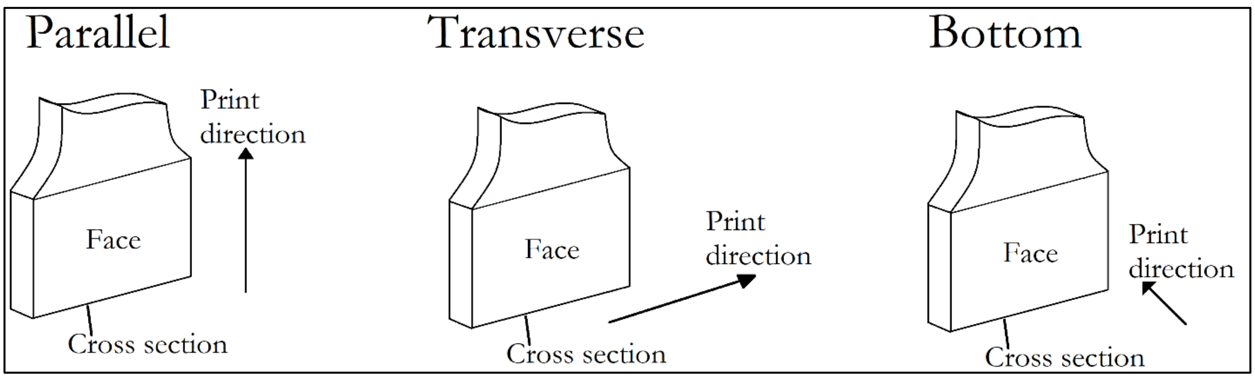

Figure 6.—Schematic showing the three print directions for tensile samples and how this relates to the orientation (plane being viewed) of the metallographic samples. Left: parallel samples, middle: transverse samples, and right: bottom samples.

Metallography gives a representative image of the metal's microstructure free from cold working or other processing damage. The following procedure was used for each sample:

1. Section metallographic samples from the tested tensile samples using an abrasive metallography saw.

2. Cold mount in epoxy and harden for a minimum of 24 hours.

3. Grind from coarser to finer grits:

    a. 180 grit for 1 minute of grinding
    b. 320 grit for 1 minute of grinding
    c. 400 grit for 3 minutes of grinding
    d. 600 grit for 5 minutes of grinding

4. Polish to a mirror finish:

    a. 6-micron diamond polish for 5 minutes
    b. 1-micron diamond polish for 5 minutes

5. Etch with glyceregia (1:2:3 ratio of nitric acid, glycerol, and hydrochloric acid) for 80 seconds.

6. Image at the following magnifications using an optical microscope:

    a. 20X
    b. 50X
    c. 100X

Density Measurement

Density measurements were performed on one half of the broken tensile test samples. Sample densities were tested using ASTM B962-17, "Standard Test Methods for Density of Compacted or Sinter Powder Metallurgy (PM) Products Using Archimedes' Principle" (ASTM International, 2017).

Hardness Testing

Extra cube material was machined in strips from vertical and horizontal edges of the cube faces for hardness testing. Hardness testing was completed using ASTM E18-20, "Standard Test Methods for Rockwell Hardness of Metallic Materials" (ASTM International, 2020). A Rockwell hardness testing machine equipped with a 1/16-inch indenting ball was used to measure hardness (Hardness Rockwell B [HRB]). Hardness data were collected traversing both the horizontal (X or Y) and vertical (Z) print directions at 0.25-inch increments.

Tensile Performance

Tensile testing was performed at room temperature with a constant strain rate of 0.0625-inch per minute. Sample geometry was in accordance with subsize samples listed in ASTM E8/E8M-21, "Standard Test Methods for Tension Testing of Metallic Materials" (ASTM International, 2021). The samples were taken from the locations and orientations shown in figure 5 and sample nomenclature can be found in table 2. Sample orientations are relative to print direction. For comparison, four wrought 316L stainless steel samples were also tested. For the wrought samples, two groups of samples were taken at 90 degrees relative to each other and given "T" and "L" designations. Note that these do not correlate to transverse and parallel directions; the designations only serve to differentiate the sample groups.

Stress was measured using a calibrated load cell while strain was measured using an extensometer. Total elongation was evaluated in two ways: 1) as a physical measurement (length of the samples after breaking compared to the initial length) and 2) as the maximum strain. Yield stress was determined by the 0.2-percent (%) offset method, which takes the slope of the stress-strain curve's linear region (the elastic modulus) and generates a line offset by 0.2% strain. The intersection of that line with the stress-strain curve represents the transition from elastic to plastic deformation, which is the material's yield strength.

Table 2.—Tensile Sample Identification Nomenclature

First Digit Wall Designation	Second Digit Sample Orientation	Third Digit Sample Number
B = Bottom plate 1/2 = 1/2-inch wall 1/4 = 1/4-inch wall	T = Transverse P = Parallel	Unique and sequential identification

Fractographic Analysis

For fractographic analysis, researchers captured macro images of the tensile sample fracture surfaces with a DSLR camera. Image lighting was adjusted to highlight fracture features.

Impact Performance

Charpy impact testing quantifies the energy absorbed by a material during fracture after sudden impact. For this study, impact testing utilized a "V notch" standard sample geometry in accordance with ASTM E23-18, "Standard Test Methods for Notched Bar Impact Testing of Metallic Materials" (ASTM International, 2018). The samples were taken from the locations and orientations shown in figure 5 and sample nomenclature can be found in table 3. Sample notch orientations are relative to print direction. All samples were tested at room temperature.

Table 3.—Impact Sample Identification Nomenclature

First Digit Sample Notch Orientation	Second Digit Sample Number
T = Transverse P = Parallel	Unique and sequential identification

Results and Analysis

Dimensional Analysis

An important feature of the AM process is how well the printed piece complies with dimensional tolerances. To quantify this, researchers performed a 3D laser scan, recreating the surface of the printed cube as a 3D model and comparing it against the computer-aided design model used for the print. The 3D Laser Scan Results are included in appendix B. These results show that the PBF-produced cube closely aligned with the computer-aided design model.

Metallographic Analysis

Microstructures from each sample orientation can be seen in figures 7 through 13. All samples display a characteristic columnar grain structure within the weld beads [1]. Metals in their solid form are usually polycrystalline, and grains are the individual crystals within that, which have a uniform structure [2]. Grain size is consistent throughout the samples and the shape of the grains are elongated parallel to the print direction. The elongation is readily observable in the transverse cross section sample shown in figure 12. Frequently, grains maintained the same orientation to the grains within adjacent weld beads. Micrographs displaying the X-Z and Y-Z planes show a similar grain shape and elongation to one another.

Porosity is present, as evidenced by small, dark spots in light-field micrographs and bright spots in dark-field micrographs, though only in a relatively small area fraction. This is a result of the laser power parameters used; porosity has been shown to decrease with increased laser power [3]. Impurities are not readily seen in any of the micrographs, indicating purity of the starting powder. No notable differences were observed between material taken from the 1/4-inch and 1/2-inch walls, indicating that heat input was roughly equivalent.

Overall, the melt parameters used to produce these parts resulted in a grain size/shape consistent with the literature on PBF-produced 316 stainless steel [1, 3, 4].

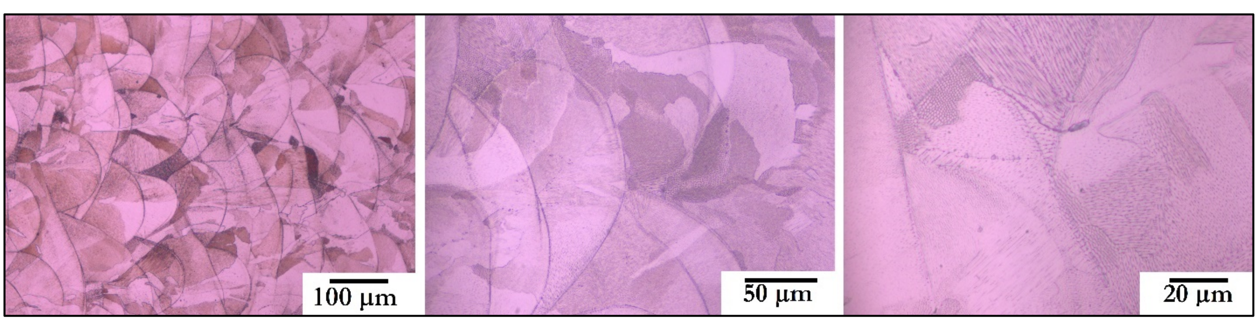

Figure 7.—Microstructure of sample 1/2P1F.

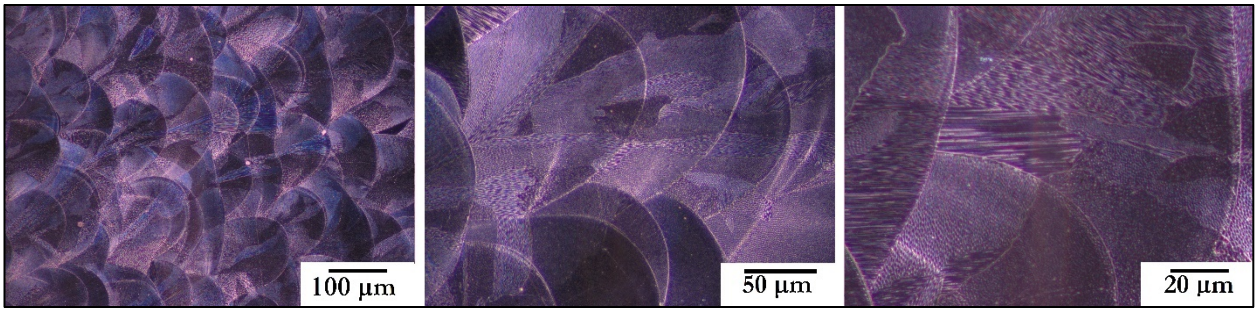

Figure 8.—Microstructure of sample 1/2P1X.

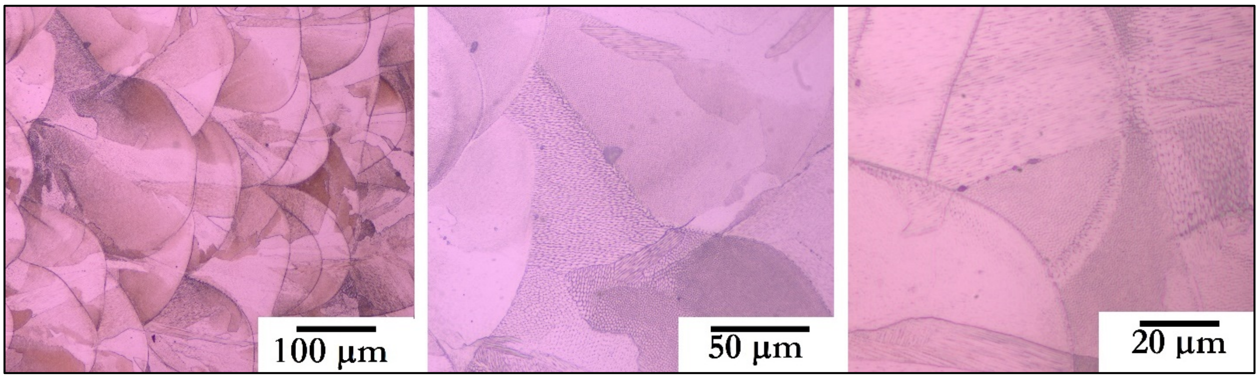

Figure 9.—Microstructure of sample 1/4P1F.

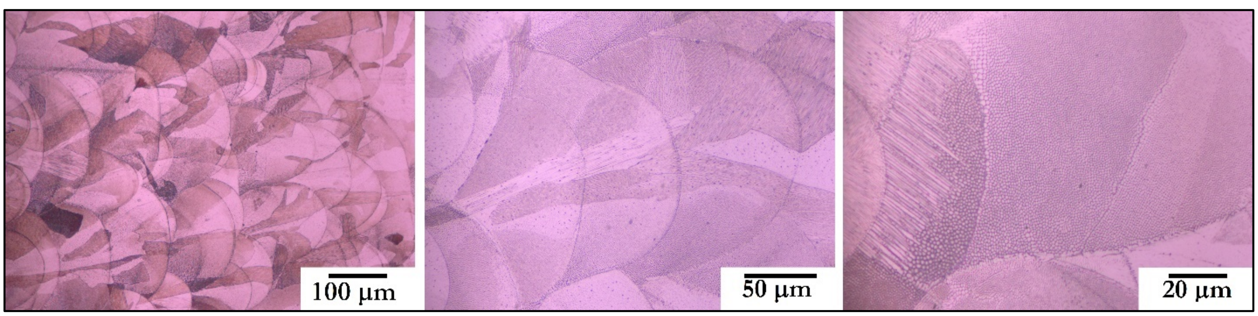

Figure 10.—Microstructure of sample 1/4P1X.

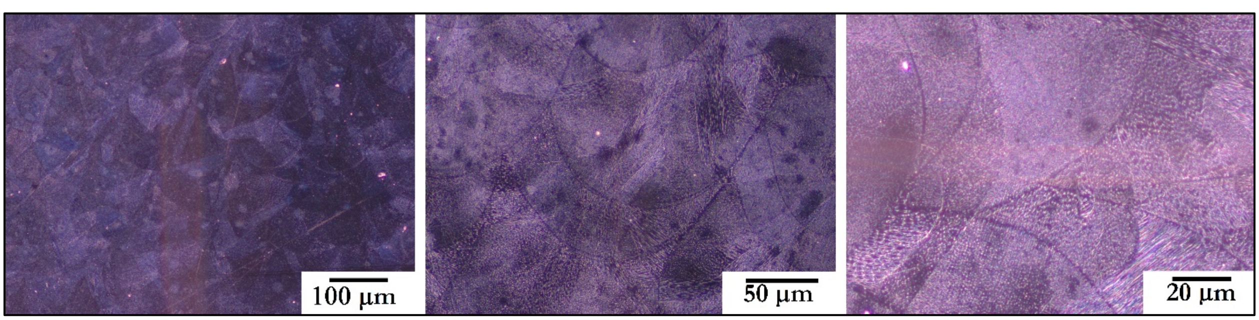

Figure 11.—Microstructure of sample 1/4T1F.

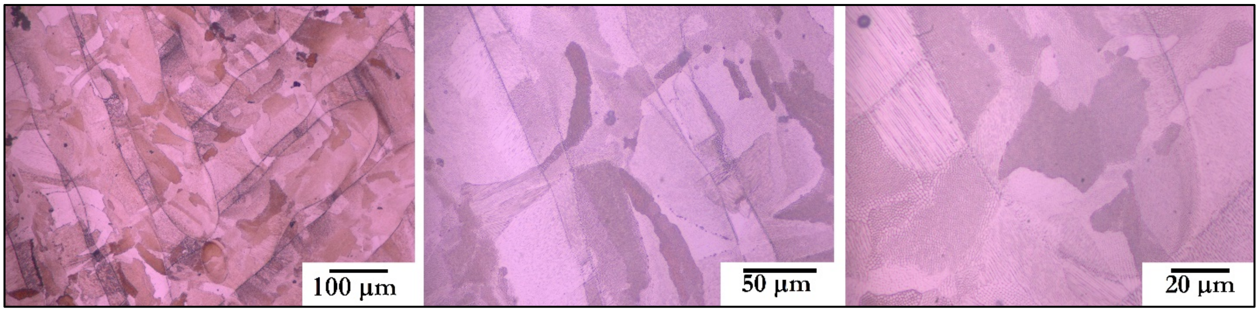

Figure 12.—Microstructure of sample 1/4T1X.

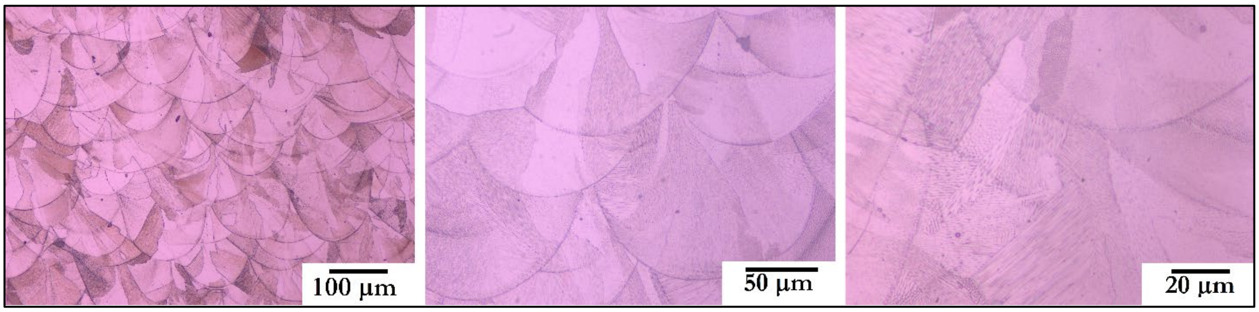

Figure 13.—Microstructure of sample B1X.

Density Measurement

Density measurements are shown in table 4. With the exception of sample 1/2P3, all samples were in the 96 to 97% dense range. This indicates that the starting material was adequately sized and that melt parameters were optimal for this process. Improperly sized starting powder can lead to larger voids between particles; likewise, insufficient melting parameters can also lead to voids between partially melted powder particles. For most applications, voids are unfavorable due to their detrimental impact on mechanical properties [5, 6]. Additionally, porosity generally has a negative influence on corrosion resistance, though further testing would be required to quantify the effect.

Table 4.—Density Measurement Results

Sample	Density (%)
1/2T2	97.26
1/2T3	97.18
1/2P2	96.12
1/2P3	85.87
1/4P2	96.87
1/4P3	97.02
1/4T2	96.89
1/4T3	96.70
B2	96.94
B3	96.71

Hardness Testing

Hardness traverse results can be seen in figures 14 and 15. In both vertical and horizontal hardness traverses, results lie between 60 and 90 HRB. The average hardness was 80.9 HRB and 77.6 HRB for the vertical and horizontal hardness traverses, respectively. In the vertical hardness traverse, two hardness bands can be seen between 80 and 90 HRB, and between roughly 65 and 75 HRB. The difference in these bands may be correlated with interlayer bonding, where the higher band represents a hardness test point located more centered within a single layer, and the lower band represents a hardness test point that was located more centered between layers. From a performance perspective, the non-uniformity in hardness could lead to a reduction in wear performance at a local level or uneven wear at macroscopic level, depending on the part, wear surface, and loading and orientation. Further testing would be required to quantify the impact.

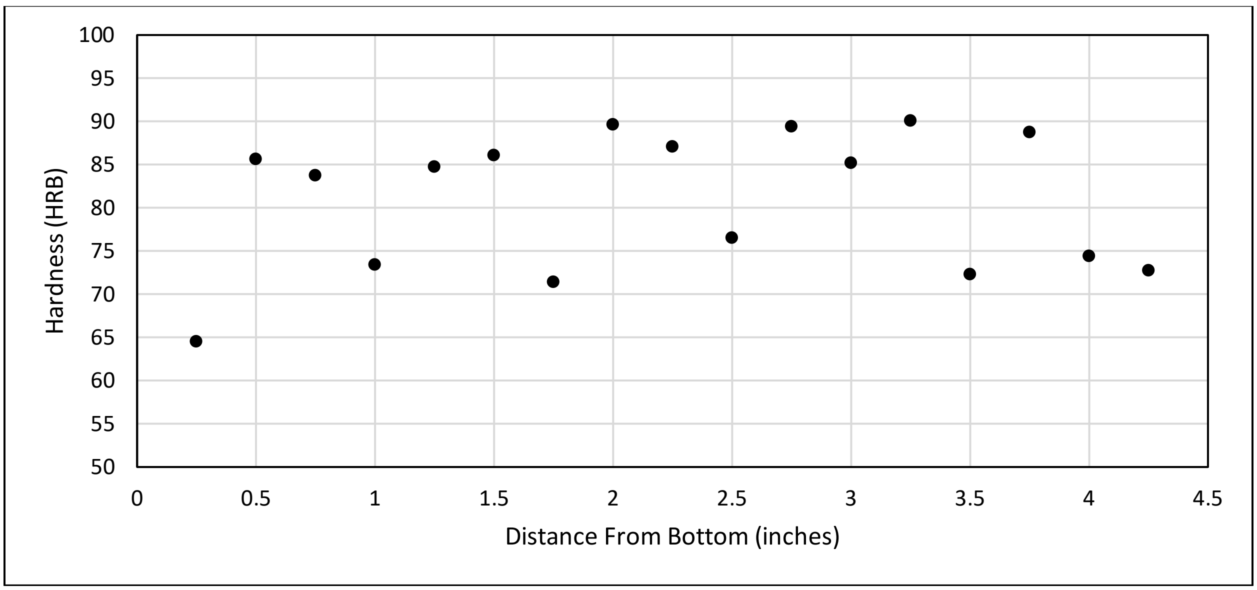

Figure 14.—Plot of hardness measurements taken in the vertical, Z, direction.

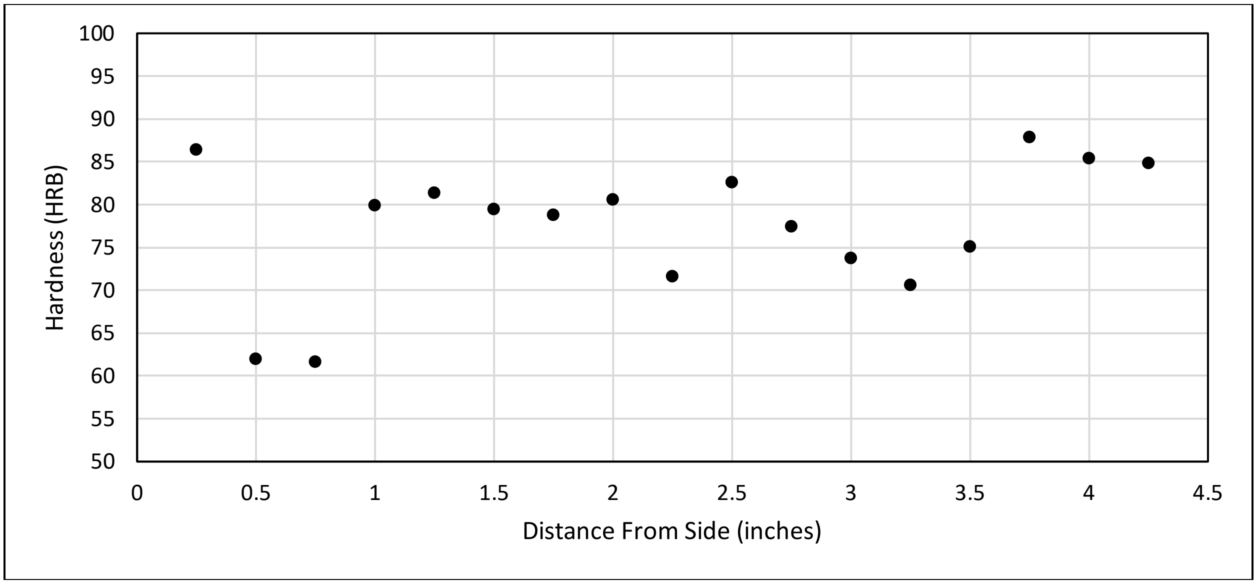

Figure 15.—Plot of hardness measurements taken in the horizontal, X or Y, direction.

Tensile Performance

Complete sets of tensile test results in the form of stress-strain curves can be seen in figures 16 through 18. Figure 19 shows the test results from samples machined from a plate of wrought 316L stainless steel. Key data from the graphs is summarized in the following sections for yield stress, ultimate tensile strength (UTS), and elongation, as well as statistical analysis. All tensile data are tabulated in appendix C.

Tensile Testing Results

Generally, the stress-strain curves show that 1/4-inch and 1/2-inch wall samples taken parallel to the print direction exhibit a higher UTS and lower elongation than those taken transverse to the print direction. The graphs also show distinct cohorts comprised of the transverse and parallel samples, indicating anisotropy in performance due to the print/build orientation.

All additively manufactured samples had lower elongations compared to the wrought samples. Parallel and bottom plate samples displayed higher UTS values, while transverse samples displayed lower UTS values compared to the wrought samples.

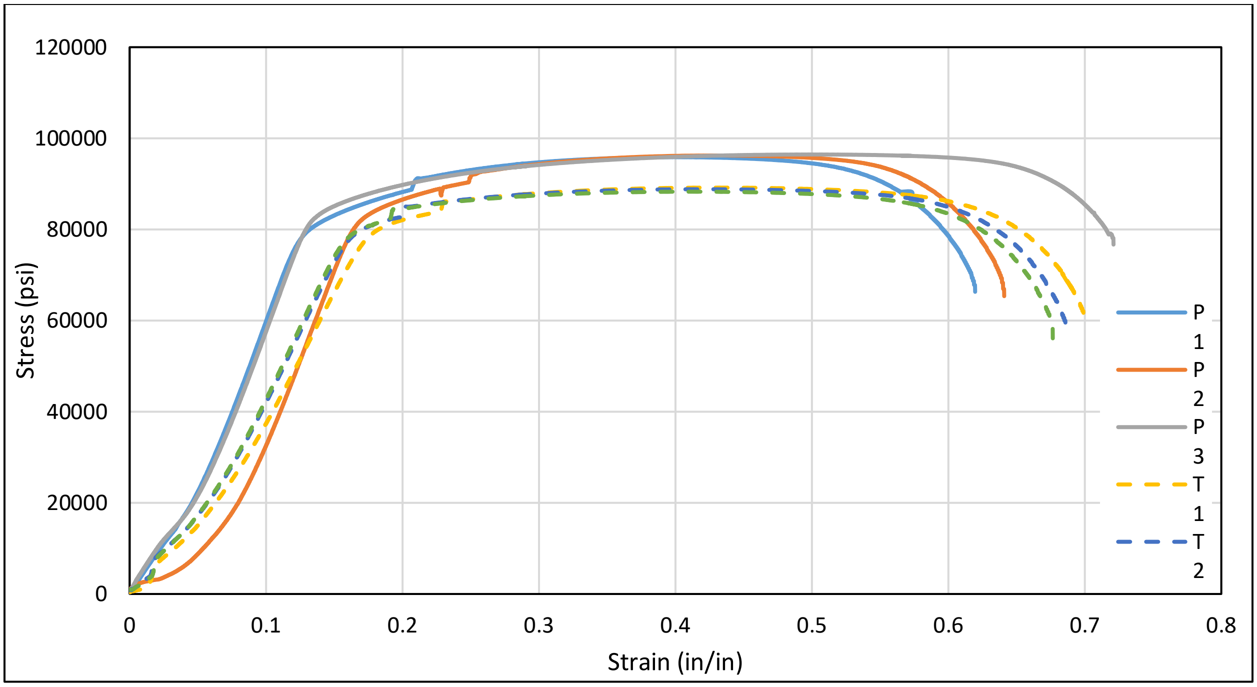

Figure 16.—Tensile test results of PBF 316L stainless steel samples taken from the 1/4-inch wall.

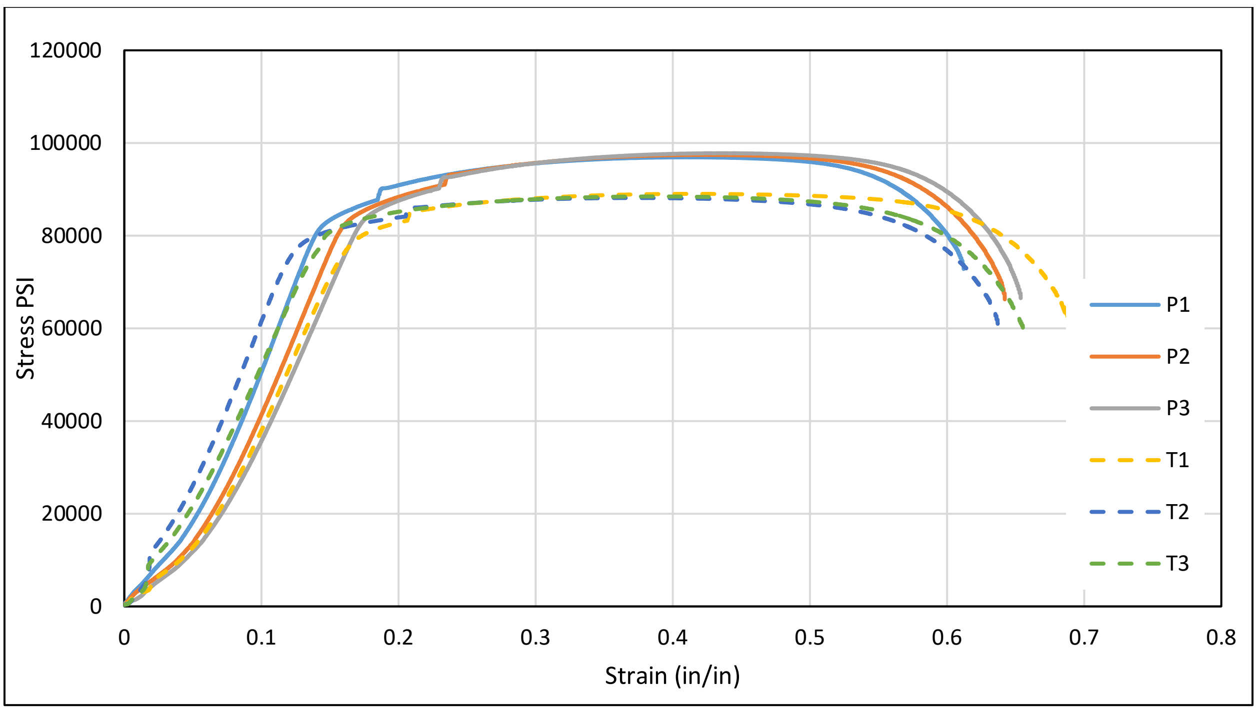

Figure 17.—Tensile test results of PBF 316L stainless steel samples taken from the 1/2-inch wall.

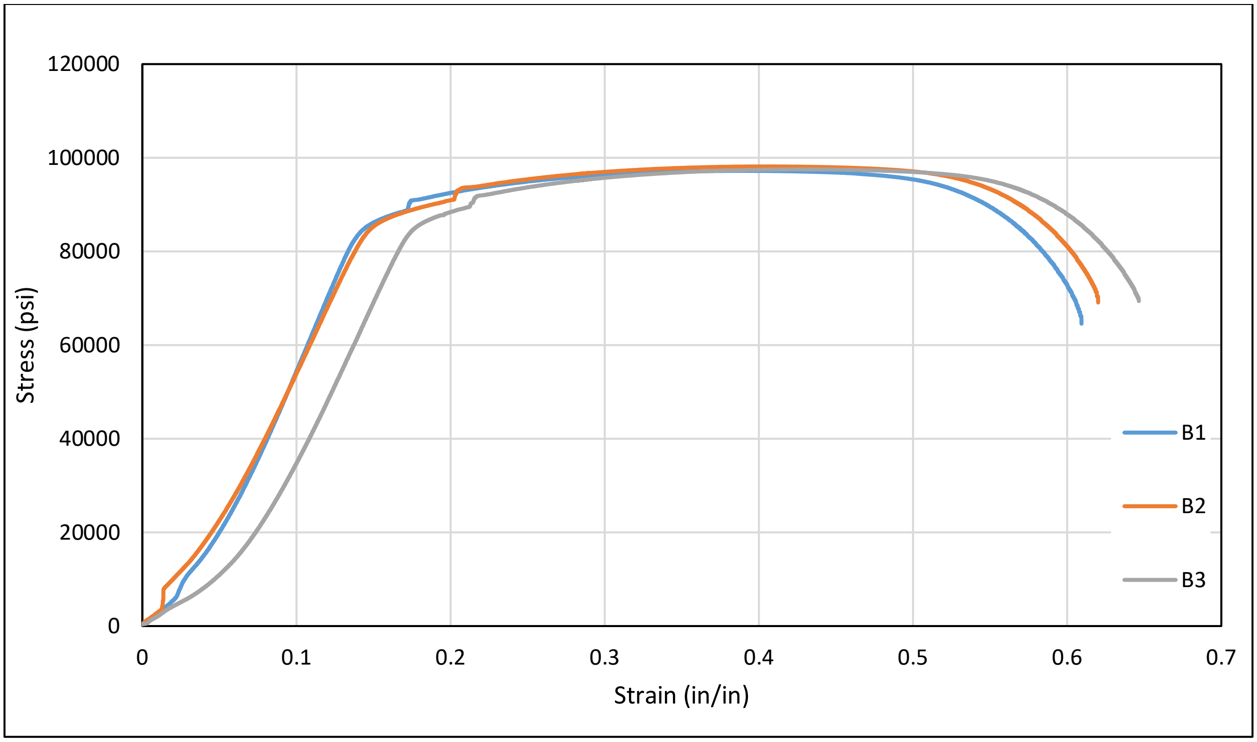

Figure 18.—Tensile test results of samples taken from the bottom plate.

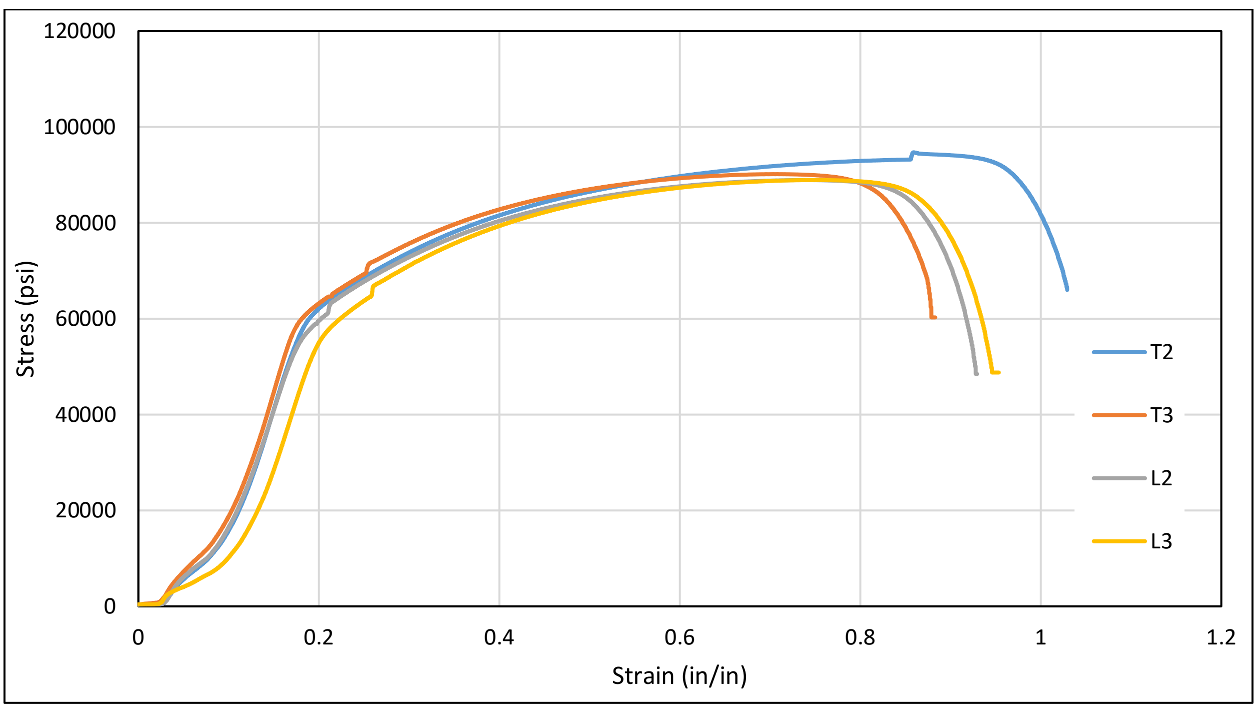

Figure 19.—Tensile test results of samples taken from a wrought plate.

Yield Stress Results

Yield stress results from tensile testing are summarized in table 5. The average yield stress of the PBF samples was 74,800 pounds per square inch (psi), which is higher than the average yield strength of the wrought material (49,000 psi). This could be due to differences in grain size and/or thermal processing; however, further testing would be needed to determine the exact cause. Among the PBF samples, the parallel and bottom samples displayed the highest yield stress. The transverse samples displayed the lowest yield stress, which can likely be attributed to interlayer bonding. For transverse samples, tension was applied such that layers were being pulled apart. In contrast, in parallel samples, tension was applied such that the layers were being pulled much like a bundle of wires.

The difference in average yield stress between 1/4-inch and 1/2-inch wall samples was statistically insignificant, indicating minimal differences in heat input due to the difference in mass. Standard deviation in yield stress, an indicator of material uniformity, was lowest in bottom plate samples and was roughly equivalent between parallel and transverse samples.

Regarding performance, the difference in yield strength between parallel and transverse samples indicates anisotropy in the material that would need to be considered along with component loading conditions and orientations before use in certain applications.

Table 5.—Summary of Yield Stress Results

Group	Average Yield Stress (psi)	Standard Deviation (psi)	Percent Standard Deviation (%)
1/4-inch Parallel	77,167	2,867	3.72
1/2-inch Parallel	74,667	1,027	1.38
Bottom Plate	78,333	236	0.30
1/4-inch Transverse	70,000	1,080	1.54
1/2-inch Transverse	73,833	2,055	2.78
Wrought "T"	50,850	N/A	N/A
Wrought "L"	47,150	N/A	N/A
Literature (316L Plate)	34,100 [7]	N/A	N/A

Ultimate Tensile Strength

UTS results are summarized in table 6. The average UTS for all PBF samples was 93,700 psi, which is higher than annealed plate material with a UTS of around 75,000 to 82,000 psi [7, 8] and consistent with literature for PBF 316L material [1, 4]. When broken up by sample group, there is some variation in average UTS. The parallel and bottom plate samples had higher UTS, whereas the transverse samples had notably lower UTS, closer in value to, but below, the wrought samples. As with the lower yield stress observed in transverse samples, the lower UTS can likely also be attributed to interlayer bonding. Standard deviations in UTS were consistently lower than those of the yield stresses, with the lowest standard deviation occurring in the parallel samples. No notable differences in UTS were observed between the 1/4-inch and 1/2-inch wall samples.

The difference in UTS between parallel and transverse samples displays the same anisotropy and, as previously noted, that would need to be considered before use in some applications.

Table 6.—Summary of UTS Results

Group	Average UTS (psi)	Standard Deviation (psi)	Percent Standard Deviation (%)
1/4-inch Parallel	96,167	236	0.25
1/2-inch Parallel	97,500	408	0.42
Bottom Plate	97,500	408	0.42
1/4-inch Transverse	88,833	236	0.27
1/2-inch Transverse	88,500	408	0.46
Wrought "T"	92,250	N/A	N/A
Wrought "L"	88,920	N/A	N/A
Literature (316L Plate)	81,200 [7]	N/A	N/A

Elongation

Elongation results are shown in table 7. The parallel samples had slightly lower percent elongation than the transverse samples. The bottom plate samples had the lowest average elongation of all samples. The wrought samples had the highest average percent elongation of all samples.

While the lower elongation observed in PBF samples relative to wrought samples is concerning regarding comparable performance, the samples still averaged roughly 47% elongation by physical measurement. Elongation provides an indication of material's ability to withstand plastic deformation without fracturing. In practice, this amounts to a component bending or stretching before breaking, potentially providing time for damage to be observed prior to failure of the component.

Table 7.—Elongation Measurements

Group	Average Percent Elongation by Physical Measurement (%)
1/4-inch Parallel	47
1/2-inch Parallel	45
Bottom Plate	43
1/4-inch Transverse	49
1/2-inch Transverse	49
Wrought "T"	61.5
Wrought "L"	63
Literature (316L Plate)	55 [7]

Fractographic Analysis

Representative macro images of the fractography results from tested tensile samples are shown in figure 20. For all samples, there is a region surrounding the fracture surface that shows a reduction in the cross-sectional area. This region is produced prior to failure and is known as "necking." There are also regions of shear failure along the edges of the samples. These regions are typically the last to form (immediately prior to complete fracture) and approach 45 degrees from the axis of applied tensile stress, parallel to the plane of maximum shear stress. These observations indicate a cup-and-cone type fracture that is typical of ductile failure. It is notable that no material defects or voids were observed in the macro images, which is a good indication of starting material purity and optimal build parameters being used.

For structural applications, a ductile mode of fracture is often preferable to brittle failure. Brittle failures are characterized by fracture features that are almost entirely "flat" or perpendicular to the axis of applied stress, and do not show significant necking. As previously noted, ductility is useful in that it provides more opportunity for damage to be detected prior to complete failure, whereas brittle failures tend to occur rapidly.

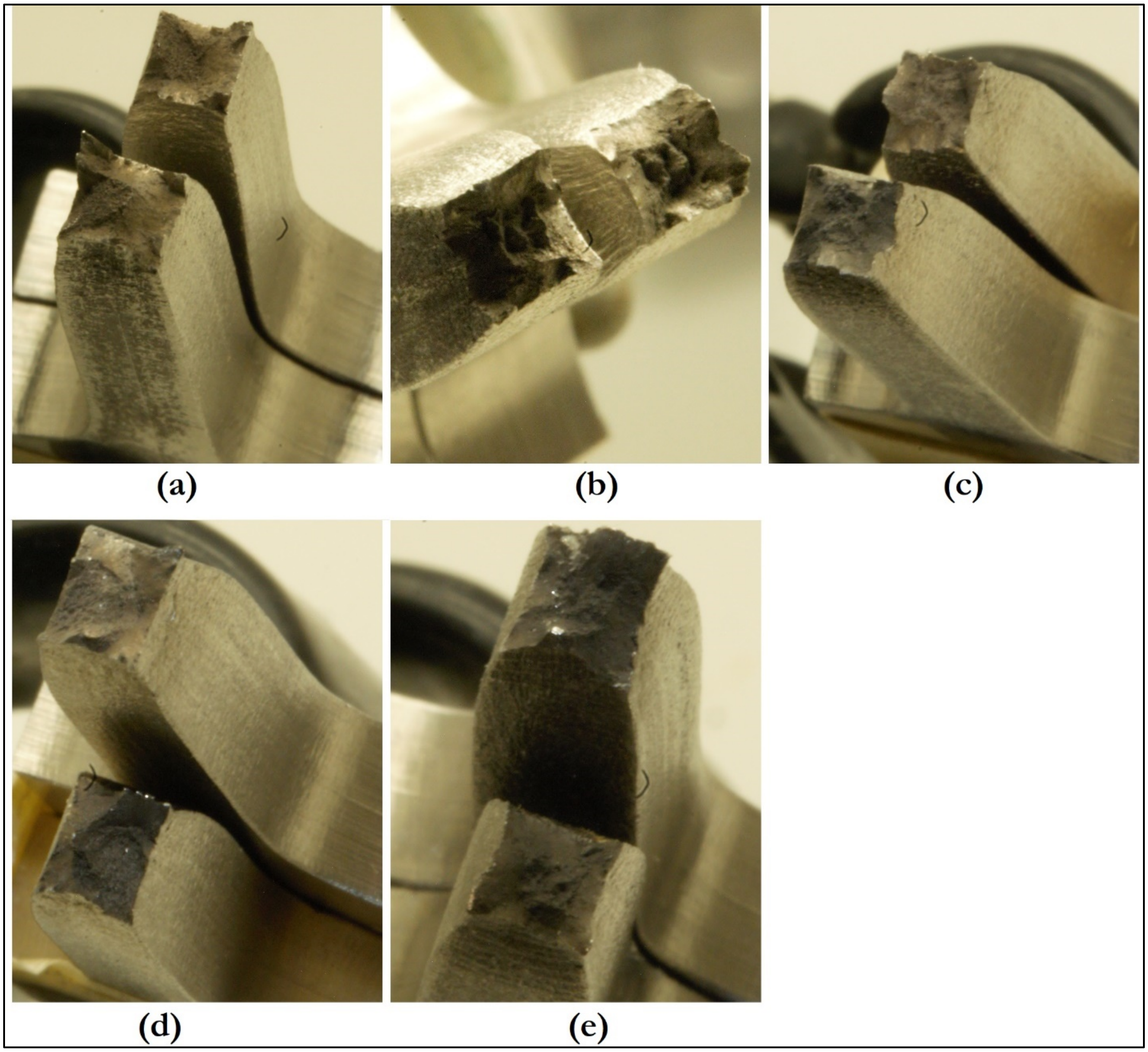

Figure 20.—Fractography of tested tensile samples representative of [a] 1/4-inch parallel samples, [b] 1/4-inch transverse samples, [c] bottom samples, [d] 1/2-inch parallel samples, and [e] 1/2-inch transverse samples.

Impact Performance

Charpy impact results are tabulated in table 8. Transverse samples displayed a slight decrease in impact performance compared with parallel samples, indicating a small degree of anisotropy due to the manufacturing process. Overall results were consistent within sample groups indicating the material was relatively free of defects.

Table 8.—Impact Testing Results

Sample	Charpy Impact Energy (foot-pounds)
P1	122
P2	124
P3	123
Average:	**123**
T1	114
T2	118
T3	120
Average:	**117**
Literature (wrought):	180-350 [9]

Representative images of broken impact samples can be seen in figure 21. Large fibrous regions are observed in the samples that are associated with shear facture. The contraction of the material at the notch of the samples indicates ductility.

The Charpy impact energy results and fracture surfaces indicate the material's toughness, or its ability to withstand stress. Literature values indicate the toughness of the PBF is lower than that of wrought material [9].

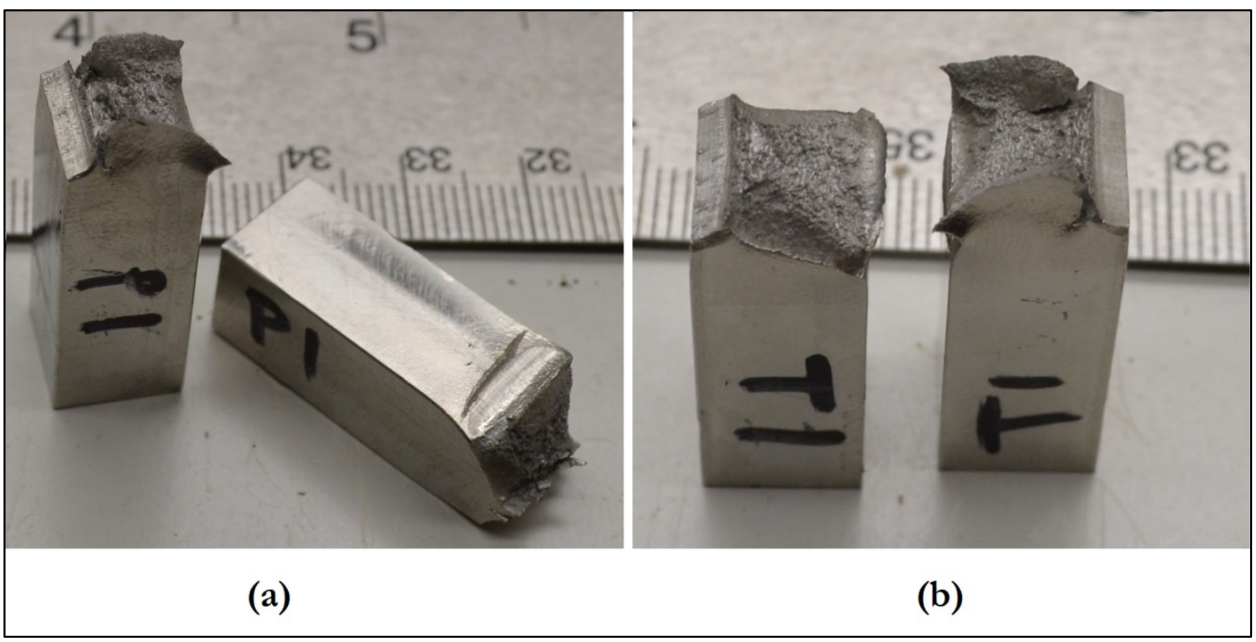

Figure 21.—Tested impact samples. Notch oriented [a] parallel and [b] transverse to print direction.

Conclusions

The results of the material performance and characteristics of PBF-produced stainless steel 316L are summarized as follows:

- The PBF process achieved high dimensional accuracy to the computer-aided design model.
- Impurities were not observed within the material, though a small amount of porosity was observed in micrographs.
- No significant differences were noted between material from the 1/2-inch and 1/4-inch walls.
- Anisotropy was most notable in the direction transverse to print layer deposition, displaying an overall reduced material performance.
- The material exhibited a lower toughness than wrought material.

With consideration of the above findings, the PBF process, when used with appropriate starting material and process parameters, may be an acceptable candidate for production of components depending on application. Consideration should be given to the orientation of components in the build process as material performance was observed to be anisotropic and, therefore, the appropriateness for use may require assessment on a case-by-case basis.

References

[1] Qui, C., M.A. Kindi, A.S. Aladawi, and I.A. Hatmi. 2018. "A Comprehensive Study on Microstructure and Tensile Behaviour of a Selectively Laser Melted Stainless Steel." *Scientific Reports* 8(1):7785, https://doi.org/10.1038/s41598-018-26136-7

[2] Reed-Hill, R.E. and R. Abbaschian. 1994. *Physical Metallurgy Principles*. Third Edition, PWS Publishing Company, Boston, Massachusetts.

[3] Choo, H., K.-L. Sham, J. Bohling, A. Ngo, X. Xiao, Y. Ren, P.J. Depond, M.J. Matthews, and E. Garlea. 2019. "Effect of Laser Power on Defect, Texture, and Microstructure of a Laser Powder Bed Fusion Processed 316L Stainless Steel ." *Materials and Design*, Volume 164, No. 107534, https://doi.org/10.1016/j.matdes.2018.12.006.

[4] Kluczynski, J., L. Sniezek, K. Grzelak, J. Janiszewski, P. Platek, J. Torzewski, I. Szachogluchowicz, and K. Gocman. 2020. "Influence of Selective Laser Melting Technological Parameters on the Mechanical Properties of Additively Manufactured Elements Using 316L Austenitic Steel,." *Materials*, Volume 13(6), No. 1449, https://doi.org/10.3390/ma13061449.

[5] Dieter, G.E. 1986. *Mechanical Metallurgy*. Third Edition. McGraw-Hill, New York, New York.

[6] ASM International. 1996. "Fatigue and Fracture." *ASM Handbook*, Volume 19. ASM International, Materials Park, Ohio, www.asminternational.org.

[7] MatWeb. (n.d.). "316 Stainless Steel, annealed plate." Available at http://www.matweb.com/search/DataSheet.aspx?MatGUID=3a413dabd215462da3408e6e8b761349. Accessed October 8, 2021.

[8] Krauss, G. 2005. *Steels: Processing, Structure, and Performance*. ASM International, Materials Park, Ohio, www.asminternational.org.

[9] Lou, X., P.L. Andresen, and R.B. Rebak. 2018. "Oxide Inclusions in Laser Additive Manufactured Stainless Steel and Their Effects on Impact Toughness and Stress Corrosion Cracking Behavior." *Journal of Nuclear Materials*, Volume 499, pp. 182-190 https://doi.org/10.1016/j.jnucmat.2017.11.036.

Additional References—ASTM Standards

ASTM International. 2021. ASTM E8/E8M-21, "Standard Test Methods for Tension Testing of Metallic Materials." West Conshohocken, Pennsylvania, www.astm.org. https://doi.org/10.1520/E0008_E0008M-21

ASTM International. 2020. ASTM E18-20, "Standard Test Methods for Rockwell Hardness of Metallic Materials." West Conshohocken, Pennsylvania, www.astm.org. https://www.astm.org/Standards/E18.htm

ASTM International. 2018. ASTM E23-18, "Standard Test Methods for Notched Bar Impact Testing of Metallic Materials." West Conshohocken, Pennsylvania, www.astm.org. https://www.astm.org/Standards/E23.htm.

ASTM International. 2017. ASTM B962-17, "Standard Test Methods for Density of Compacted or Sintered Powder Metallurgy (PM) Products Using Archimedes' Principle." West Conshohocken, Pennsylvania, www.astm.org. https://doi.org/10.1520/B0962-17

Appendix A—Powder Feedstock Documentation

LPW

Test Certificate

Customer: Concurrent Technologies Corportation
Sales Order #: 000985
Customer PO #: 180900120

Product Code: LPW-316-AAAV **Product Rev:** 01
Batch Number : US80881 **Quantity:** 230 Kg

CHEMICAL ANALYSIS

		Units	Min	Max	Result	Approved
C	Carbon	weight %	-	0.030	0.017	Y
Cr	Chromium	weight %	17.5	18.0	17.6	Y
Cu	Copper	weight %	-	0.50	0.02	Y
Fe	Iron	weight %	-	Bal	Bal	Y
Mn	Manganese	weight %	-	2.00	0.93	Y
Mo	Molybdenum	weight %	2.25	2.50	2.32	Y
N	Nitrogen	weight %	-	0.10	0.09	Y
Ni	Nickel	weight %	12.5	13.0	12.6	Y
O	Oxygen	weight %	-	0.10	0.03	Y
P	Phosphorus	weight %	-	0.025	0.009	Y
S	Sulfur	weight %	-	0.010	0.004	Y
Si	Silicon	weight %	-	0.75	0.58	Y

SIEVE ANALYSIS - ASTM B214

	Units	Min	Max	Result	Approved
+45 µm	weight %	Info Only	-	1	Y

LASER SIZE DIFFRACTION - ASTM B822

	Units	Min	Max	Result	Approved
-16 µm	volume %	Info Only	-	8.2	Y

NOTES

LPW Technology Certifies that the material on this document conforms to the specification above.
*This document is validated by suppliers authorised inspection representative in accordance with EN 10204 type 3.1 Inspection Document

Generated By	Validated By*
LPW 34	LPW 24
Date	Date
26 SepT 2018	26 Sept 2018

LPW Technology Limited is a company registered in England and Wales
Company registration: 06233481 VAT Registration Number: GB 920134667
Registered office:Dennis Road,Widnes,Cheshire WA8 0GU UK

FORM23-ISSF

Appendix B—3D Laser Scan Results for Test Cube

PolyWorks

BUREAU OF RECLAMATION	3D Metal Printed 5" box Report Author: Chad Paulson Date: 2/25/2020

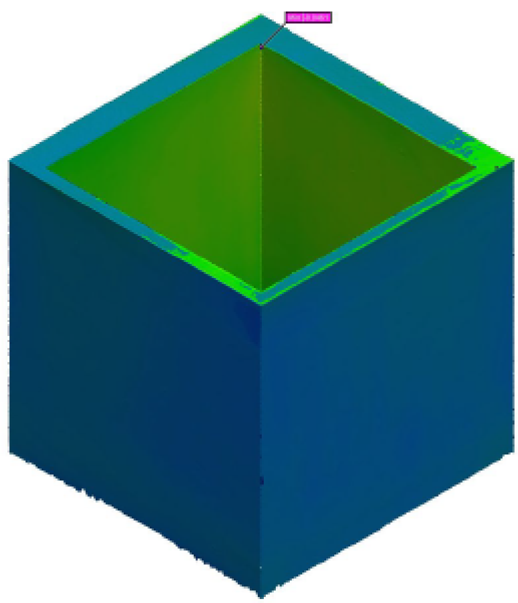

Organization:	Bureau of Reclamation	Part name:	
Operator:		Part number:	
E-mail:	cpaulson@usbr.gov	Drawing #:	
Workspace:	Stainless Box	Serial #:	
Project:	Stainless Box Scan 2 - Stainless	Device:	FARO Laser Line Probe

1/5

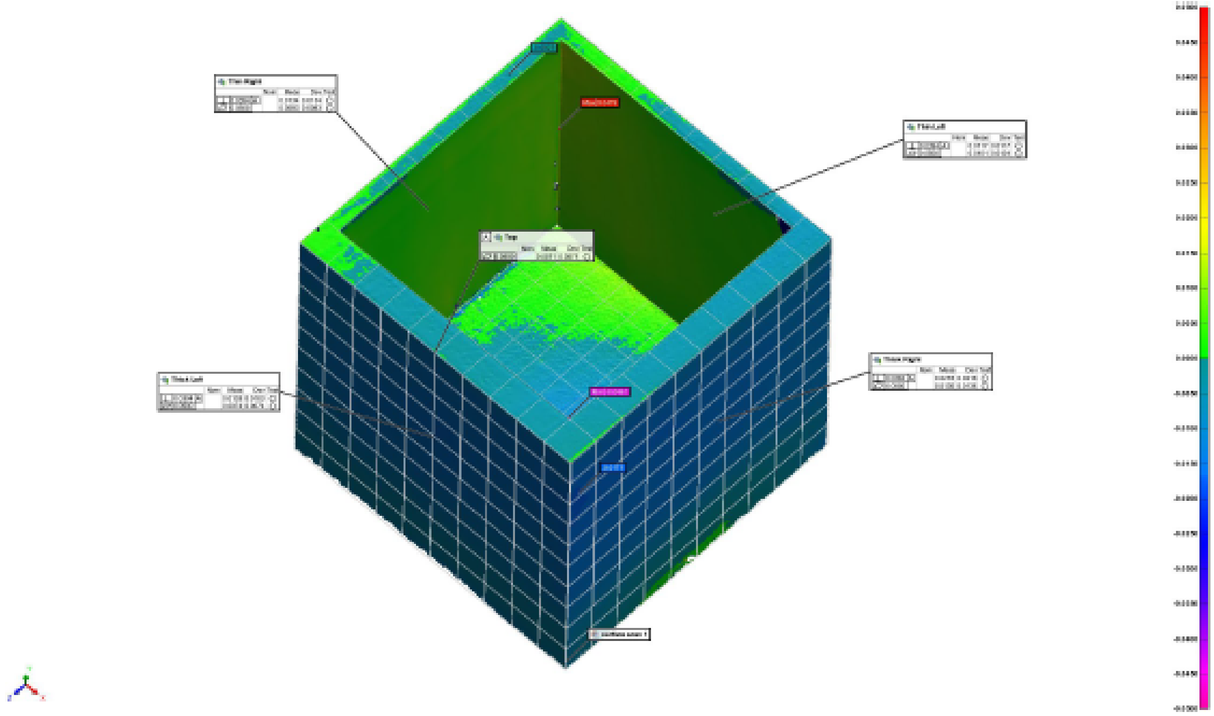

Control View

Control View Name	Isometric View
Units	Inches
Coordinate Systems	world
Data Alignments	
All Statistics	Total: 9, Measured: 9 (100.0000%), Pass: 9 (100.0000%), Fail: 0 (0.0000%), Warning: 0 (0.0000%)

Char No.	Object Name	Control	Nom	Meas	Tol	Dev	Test	Out Tol
	Top	⏥ 0.0500		0.0071	0.0500	0.0071	Pass	
	Thick Right	⊥ 0.0394 A		0.0218	0.0394	0.0218	Pass	
	Thick Right	⏥ 0.0500		0.0136	0.0500	0.0136	Pass	
	Thick Left	⊥ 0.0394 A		0.0103	0.0394	0.0103	Pass	
	Thick Left	⏥ 0.0500		0.0074	0.0500	0.0074	Pass	
	Thin Left	⊥ 0.0394 A		0.0117	0.0394	0.0117	Pass	
	Thin Left	⏥ 0.0500		0.0101	0.0500	0.0101	Pass	
	Thin Right	⊥ 0.0394 A		0.0134	0.0394	0.0134	Pass	
	Thin Right	⏥ 0.0500		0.0083	0.0500	0.0083	Pass	

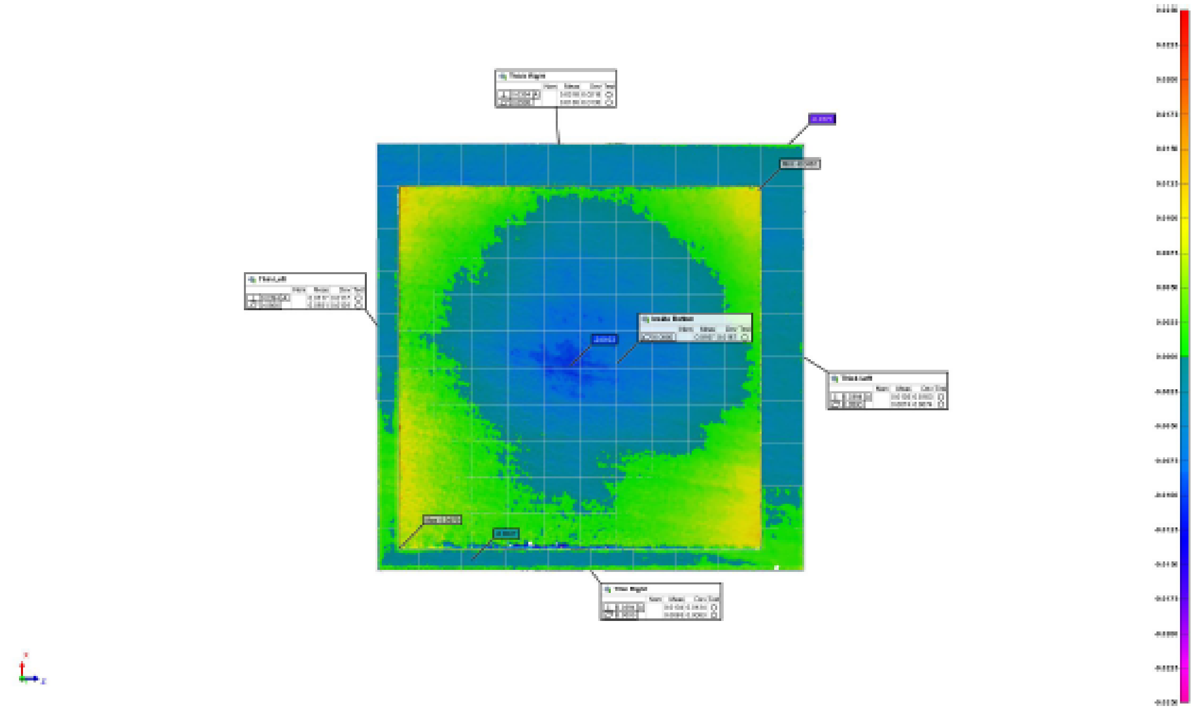

Control View

Control View Name	Top View
Units	Inches
Coordinate Systems	world
Data Alignments	
All Statistics	Total: 9, Measured: 9 (100.0000%), Pass: 9 (100.0000%), Fail: 0 (0.0000%), Warning: 0 (0.0000%)

Char No.	Object Name	Control	Nom	Meas	Tol	Dev	Test	Out Tol
	Thick Right	⊥ 0.0394 A		0.0218	0.0394	0.0218	Pass	
	Thick Right	▱ 0.0500		0.0136	0.0500	0.0136	Pass	
	Thick Left	⊥ 0.0394 A		0.0103	0.0394	0.0103	Pass	
	Thick Left	▱ 0.0500		0.0074	0.0500	0.0074	Pass	
	Thin Left	⊥ 0.0394 A		0.0117	0.0394	0.0117	Pass	
	Thin Left	▱ 0.0500		0.0101	0.0500	0.0101	Pass	
	Thin Right	⊥ 0.0394 A		0.0134	0.0394	0.0134	Pass	
	Thin Right	▱ 0.0500		0.0083	0.0500	0.0083	Pass	
	Inside Bottom	▱ 0.0500		0.0167	0.0500	0.0167	Pass	

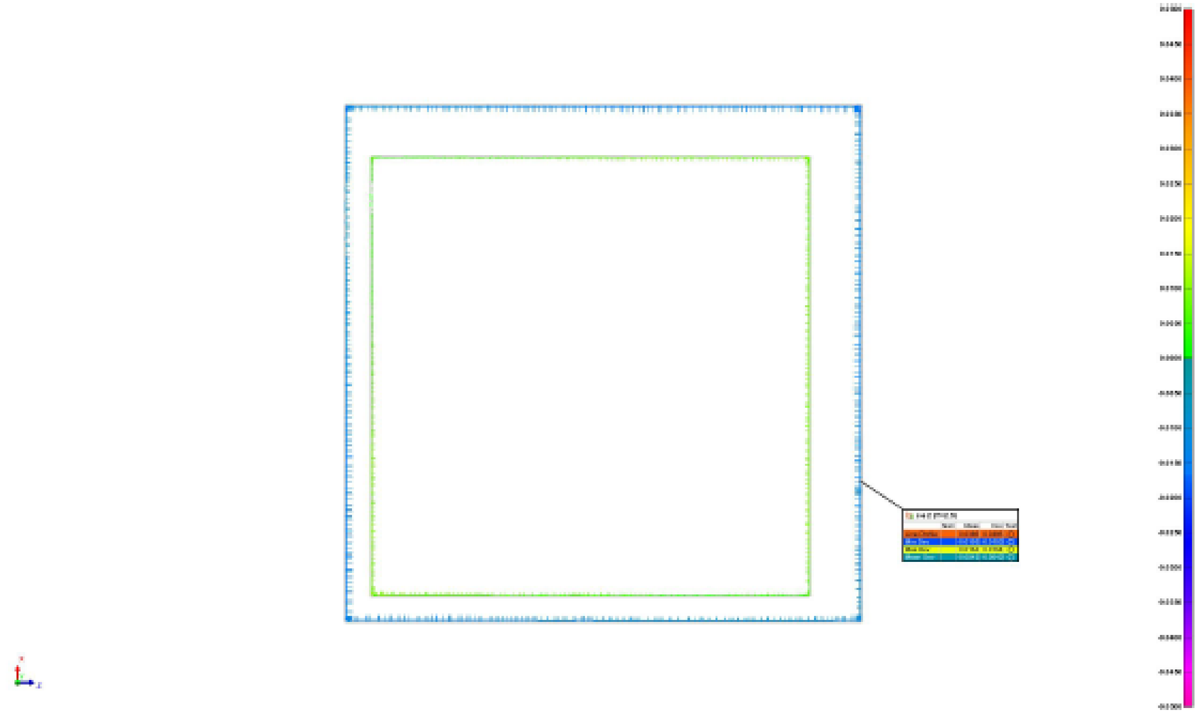

Control View

Control View Name	Top Cross Section Y=2.5
Units	Inches
Coordinate Systems	world
Data Alignments	best-fit to ref Point Pairs
All Statistics	Total: 4, Measured: 4 (100.0000%), Pass: 4 (100.0000%), Fail: 0 (0.0000%), Warning: 0 (0.0000%)

Char No.	Object Name	Control	Nom	Meas	Tol	Dev	Test	Out Tol
	c-s 2 (Y=2.5)	Line Profile		0.0385	±0.0394	0.0385	Pass	
	c-s 2 (Y=2.5)	Min Deviation		-0.0193	±0.0394	-0.0193	Pass	
	c-s 2 (Y=2.5)	Max Deviation		0.0164	±0.0394	0.0164	Pass	
	c-s 2 (Y=2.5)	Mean Deviation		-0.0043	±0.0394	-0.0043	Pass	

PolyWorks

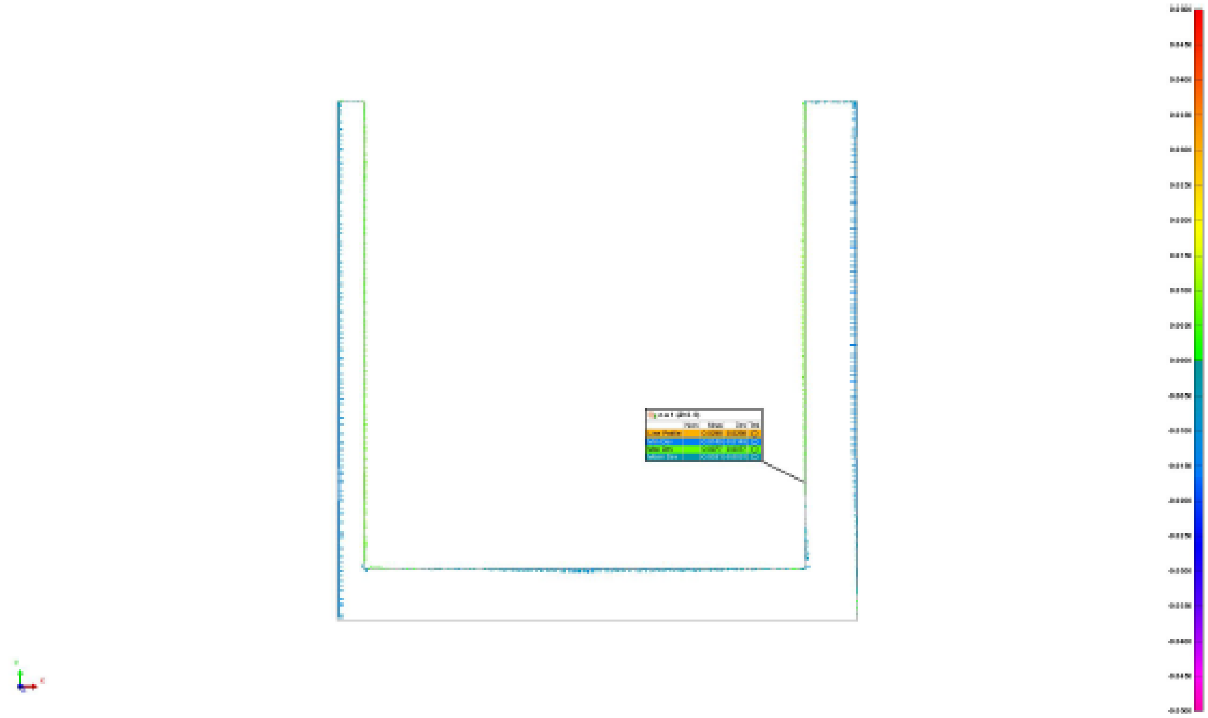

Control View

Control View Name	Side Cross Section Z=2.5
Units	inches
Coordinate Systems	world
Data Alignments	best-fit to ref Point Pairs
All Statistics	Total: 4, Measured: 4 (100.0000%), Pass: 4 (100.0000%), Fail: 0 (0.0000%), Warning: 0 (0.0000%)

Char No.	Object Name	Control	Nom	Meas	Tol	Dev	Test	Out Tol
	c-s 1 (Z=2.5)	Line Profile		0.0298	±0.0394	0.0298	Pass	
	c-s 1 (Z=2.5)	Min Deviation		-0.0149	±0.0394	-0.0149	Pass	
	c-s 1 (Z=2.5)	Max Deviation		0.0077	±0.0394	0.0077	Pass	
	c-s 1 (Z=2.5)	Mean Deviation		-0.0031	±0.0394	-0.0031	Pass	

Appendix C—Tabulated Test Results

Powder Bed Fusion

Sample	Width (in)	Thickness (in)	Area (in^2)	Yield Load (lb)	Yield Stress (psi)	Ultimate Tensile Load (lb)	UTS (psi)	Elongation (in)	Elongation %
1/4P1	0.2470	0.2455	0.061	4,468	73,500	5,826	96,000	1.44	44%
1/4P2	0.2455	0.2450	0.060	4,658	77,500	5,788	96,000	1.44	44%
1/4P3	0.2455	0.2455	0.060	4,839	80,500	5,814	96,500	1.52	52%
1/2P1	0.2450	0.2530	0.062	5,440	73,500	6,007	97,000	1.45	45%
1/2P2	0.2455	0.2540	0.062	4,638	74,500	6,076	97,500	1.45	45%
1/2P3	0.2455	0.2530	0.062	4,706	76,000	6,074	98,000	1.45	45%
B1	0.2500	0.2540	0.064	4,995	78,500	6,173	97,000	1.42	42%
B2	0.2490	0.2540	0.063	4,945	78,000	6,168	97,500	1.44	44%
B3	0.2475	0.2530	0.063	4,823	78,500	6,146	98,000	1.43	43%
1/4T1	0.2455	0.2270	0.056	3,823	70,500	4,971	89,000	1.49	49%
1/4T2	0.2455	0.2400	0.059	4,022	68,500	5,234	89,000	1.49	49%
1/4T3	0.2465	0.2355	0.058	4,127	71,000	5,126	88,500	1.49	49%
1/2T1	0.2465	0.2520	0.062	4,556	73,500	5,530	89,000	1.49	49%
1/2T2	0.2455	0.2485	0.061	4,369	71,500	5,378	88,000	1.49	49%
1/2T3	0.2455	0.2535	0.062	4,750	76,500	5,506	88,500	1.49	49%

Wrought

Sample	Width (in)	Thickness (in)	Area (in^2)	Yield Load (lb)	Yield Stress (psi)	Ultimate Tensile Load (lb)	UTS (psi)	Elongation (in)	Elongation %
T2	0.2455	0.2460	0.060	2,943	48,700	5,719	94,700	1.68	68%
T3	0.2455	0.2460	0.060	3,214	53,000	5,445	90,150	1.55	55%
L2	0.2450	0.2455	0.060	3,081	51,000	5,346	88,920	1.63	63%
L3	0.2455	0.2460	0.060	2,612	43,300	5,370	88,920	1.63	63%